




Article

Adsorption of Heavy Metals from Low Concentration Solutions onto Dried *Chlamydomonas reinhardtii*

Maria Giuseppina Genduso ^{1,*}, Marianna Guagliano ¹, Elisabetta Finocchio ², Cinzia Cristiani ¹, Giovanni Dotelli ¹ and Giulia Santomauro ³

¹ Department of Chemistry, Materials and Chemical Engineering “Giulio Natta”, Politecnico di Milano, Piazza Leonardo da Vinci 32, 20133 Milano, Italy; marianna.guagliano@polimi.it (M.G.); cinzia.cristiani@polimi.it (C.C.); giovanni.dotelli@polimi.it (G.D.)

² Department of Chemical and Process Engineering, University of Genoa, Via Opera Pia 15, 16145 Genoa, Italy; elisabetta.finocchio@unige.it

³ Department of Bioinspired Materials, Institute for Materials Science, University of Stuttgart, Heisenbergstraße 3, 70569 Stuttgart, Germany; giulia.santomauro@imw.uni-stuttgart.de

* Correspondence: mariagiuseppina.genduso@polimi.it

Abstract: Heavy metals, such as Pb(II), Cr(III), and Cd(II), are frequently discharged into the environment, resulting in a threat for the health of living organisms. Microalgae represent an ecological method for the removal of these pollutants. The capture capability of active and dried *Chlamydomonas reinhardtii* towards both mono-ionic and multi-ionic solutions is evaluated to study the bioremediation in low-polluted wastewaters. Several characterization techniques have been performed to study morphology, composition, and the interaction between the metals and the microalgal functional groups of the wall. The effect of the operating conditions, such as contact time and pH, is assessed; an increased contact time of 4 days did not influence the adsorption yields of Pb and Cr, but it had a negative effect on Cd adsorption, while the impact of pH was mainly affecting the chemical speciation, rather than the adsorption capability. The microalga showed a larger affinity for Pb and Cd, respectively, 80 and 76% (*w/w*) of adsorption, while only the 65% (*w/w*) of the total Cr was adsorbed, suggesting a preferential biosorption.

Keywords: bioremediation; microalgae; heavy metals; biosorption; wastewater treatment



Citation: Genduso, M.G.; Guagliano, M.; Finocchio, E.; Cristiani, C.; Dotelli, G.; Santomauro, G. Adsorption of Heavy Metals from Low Concentration Solutions onto Dried *Chlamydomonas reinhardtii*. *Appl. Sci.* **2024**, *14*, 11057. <https://doi.org/10.3390/app142311057>

Academic Editor: Francisco Javier Gutiérrez Ortiz

Received: 25 October 2024

Revised: 21 November 2024

Accepted: 24 November 2024

Published: 27 November 2024



Copyright: © 2024 by the authors. Licensee MDPI, Basel, Switzerland. This article is an open access article distributed under the terms and conditions of the Creative Commons Attribution (CC BY) license (<https://creativecommons.org/licenses/by/4.0/>).

1. Introduction

Increasing anthropogenic and industrial activity leads the water streams to be easily contaminated by a wide variety of organic and inorganic pollutants. Among other sources of environmental pollution, heavy metals (HMs, hereafter), which are toxic even at a low level of exposure, can be found in the majority of wastewaters due to their usage in many industrial branches [1–3]. In particular, the removal of Pb, Cr, and Cd is of paramount importance, since they can cause different serious pathologies such as kidney necrosis, anaemia, and hypertension [4–9]. Unlike organic substances, HMs are non-biodegradable, thus persistent [10]. HMs have a high mobility in water and they can be adsorbed to and accumulated in the environment and in living organisms such as plants and animals, causing them various disorders and health problems [11]. The spread of HMs can lead to the deterioration of agricultural land, phytotoxicity, and disequilibrium in soil microbial processes. Hence, wastewaters must be treated before their reintroduction into the environment, mainly due to the presence of HMs in low concentrations [12–15]. Furthermore, there is an increasing awareness that the prevention of emissions, rather than remediation of damage, is a more cost-effective and efficient approach for the mitigation of impacts on the environment and on human health [11].

Various methods for heavy metal removal have been proposed [16–18], for instance chemical precipitation, ion-exchange, membrane filtration, coagulation-flocculation, flotation, and electrochemical methods. However, these methods are expensive and require

high energy and the usage of harmful chemicals. Moreover, conventional methods are only feasible for high metal pollution concentrations. Adsorption presents a successful technology thanks to a wide variety of available sorbents, high recovery efficiency, fast extraction time, low cost, and low consumption of organic solvents. In this respect, common examples of sorbents are activated carbon, clay minerals, inorganic oxides, porous organic polymers, or organic-inorganic hybrid materials. However, considering the new circular and greener economy paradigm, the development of more environmental sustainable sorbents is a key point [19,20].

An innovative strategy to treat wastewater is presented by the use of microorganisms such as microalgae, being cost effective, very efficient in the presence of low metal concentrations, and, in principle, recyclable and reusable [9,10,21–26]. Microalgae are unicellular and eukaryotic microorganisms which can be solitary or colonial, some of them are able to move thanks to flagella [27]. Microalgae can be autotrophic or heterotrophic depending on the mechanism of energy production, the first one being related to photosynthesis with CO₂ consumption, while the second one to redox reactions [28]. According to [29], many factors may influence the biosorption of HMs by means of microalgae, such as the initial metal concentration, temperature, pH, time of contact, micronutrients, CO₂, light and time of lightness, stirring, and microalga characteristics, e.g., the microalga species.

The capture of heavy metals by microalgae can occur both actively or passively [30]. Passive capture occurs as biosorption of the metals on the cell surface. Active capture implies two mechanisms: first biosorption at the cell wall, via passive chemical and physical processes, and subsequently bioaccumulation inside the cell, via active transport. The HMs are then deposited in different organelles inside the cells. This last mechanism is metabolic- and energy-dependent; hence, living microalgae are more susceptible to toxicity, and environmental parameters. Bioaccumulation occurs more slowly than biosorption and, in principle, it is not reversible and more stable since the metals are accumulated in cell organelles [29]. In passive capture, the interaction occurs between the algal cell wall (negatively charged) and the metal ions (positively charged) with the functional groups present at the surface; the process is metabolic-independent, fast, and reversible [29]. Metal binding can occur with different mechanisms, such as electrostatic interaction, surface complexation, ion exchange, and precipitation, that can occur individually or in combination. During the adsorption process, the cell wall characteristics are of utmost importance. Indeed, different algal biomasses are characterised by different types of cell wall and thus, by various functional groups (-COOH, -OH, -NH₂, -SH) able to bind metal ions [31,32]. For biosorption, dried microalgae are advantageous since they are not affected by the toxicity of HMs and do not require a continuous supply of nutrients. The reversibility of biosorption on one side is an advantage, allowing for the sorbents' reusability, but, on the other hand, it could lead to instability of the capture.

The application of microalgal biomass in wastewater treatment systems should also include a systematic economic evaluation. The removal of heavy metals through an adsorption process includes the costs of production as well as, concerning the dried biomass, those of the drying process. According to [33], the operational and energy consumption costs depend on the technology chosen for harvesting and dewatering the microalgae. Of utmost importance is also the kind of cultivation used; generally, close reactors require lower operational and energetic costs than open ponds. Drying process costs can be lowered by using by-products coming from different waste streams as possible biosorbents; moreover, dried biomasses can be, in principle, easily regenerated and reused, reducing the costs of the cultivation step [34].

Different algal strains, such as *Chlorella vulgaris*, *Spirulina maxima*, *Spirulina platensis*, *Scenedesmus* sp., *Scenedesmus almeriensis*, *Chlorella sorokiniana*, *Parachlorella* sp., and *Chlamydomonas reinhardtii*, *Chlorophyceae* sp., are potentially suitable for heavy metal removal [10,23,35–43] (Table S1). Among the others, *Chlamydomonas reinhardtii* (*C. reinhardtii*, hereafter) has received lot of attention in recent years thanks to simple culture conditions and to its high tolerance to heavy metals [37,42,44]. In the literature, to determine the effect

of solid/liquid ratio among different heavy metal ions, high metal concentrations have been used [35,45].

The Best Available Techniques (BATs) reference documents of different productive sectors emissions in wastewaters, e.g., ceramic manufacturing, ferrous metals processing, and surface treatment of metals and plastics [46–48], report the industrial wastewaters pollution data (Table S2). Here, low concentrations of heavy metals are released in wastewaters. However, Italian and EU regulations impose strong limitations of HMs concentrations in water streams before their reintroduction into the environment and for human consumption (i.e., Pb < 0.005 mg/L, Cr < 0.025 mg/L, and Cd < 0.005 mg/L, [49]).

In this paper, the green microalga *C. reinhardtii* is exploited in its dried form to remove HMs from low-polluted environments. The aim of this work is to study the capture capability of dried microalgae towards low concentrations of HMs, such as Pb(II), Cr(III), and Cd(II), present in different productive sectors. Initial metal concentrations were fixed at 0.5 mg/L, 0.2 mg/L, and 0.2 mg/L, respectively, for Pb(II), Cr(III), Cd(II), and are related to real data reported by the BATs reference documents of industries such as ceramic manufacturing, ferrous metals processing, and surface treatment of metals and plastics [46–48]. Low concentration adsorption onto dried *C. reinhardtii*, with a preliminary comparison of Cd adsorption with living *C. reinhardtii*, was performed.

The biosorption of Pb(II), Cr(III), and Cd(II), in both mono-ionic and multi-ionic solutions, static environment, and room temperature, to a dried strain of *C. reinhardtii* is discussed. Moreover, the effect of the operating conditions, such as contact time and pH is assessed. Finally, a preliminary comparison of metal capture behaviour of active and dried *C. reinhardtii* is performed by contacting algal material with a solution containing Cd ions. Metal-sorbent interaction, before and after metal adsorption, is also studied by means of different techniques such as Scanning Electron Microscopy (SEM) equipped with Energy Dispersive X-ray analysis (EDX), and Fourier Transformed Infra-Red (FT-IR) spectroscopy in Attenuated Total Reflection (ATR) mode. The chemical composition of the liquid solution, before and after the treatment, was analysed by Inductively Coupled Plasma—Optical Emission Spectroscopy (ICP-OES).

2. Materials and Methods

2.1. Materials

In this study, living microalgae *C. reinhardtii* (strain 11-32b), supplied by Culture Collection of Algae of University of Göttingen (international acronym SAG), were used to prepare the biosorbent. Stock solutions of heavy metals Pb(II), Cr(III), and Cd(II), having a concentration of 1 mg/mL, were diluted with distilled water to obtain the desired concentration (respectively, 0.5 mg/L, 0.2 mg/L and 0.2 mg/L). During the experiments, the pH was adjusted through the addition of HCl (1 M) or NaOH (1 M) (supplied by Sigma-Aldrich, St. Louis, MO, USA) when necessary.

2.2. Biosorbent Cultivation and Preparation

Living microalga grew in Erlenmeyer flasks properly sealed with a gas permeable membrane to prevent contamination and assure ventilation. Growth was performed in a suitable medium, Kuhl medium, whose composition is reported in (Table S3). The growth of the microalgae occurred under a light emitting diode (LED) growth panel light AC 100–240 V with a 12:12 h light–dark cycle, and a room temperature of 20 ± 1 °C. After 1 week of cultivation, microalgae were harvested by centrifugation at 4000 rpm for 5 min and washed 3 to 5 times with MilliQ water (Arium[®] pro ultrapure water systems, Sartorius, Göttingen, Germany) to remove the culture medium. Then they were recovered and put into a freezer (−20 °C) for few hours. In the end, freeze-dried algae were obtained by means of a freeze-drying process (L10E, Dieter Piatkowski equipment, Petershausen, Germany), operating at a temperature of −50 °C for 48 h. Unit operations describing the preparation of the dried microalgae are sketched in Figure 1.

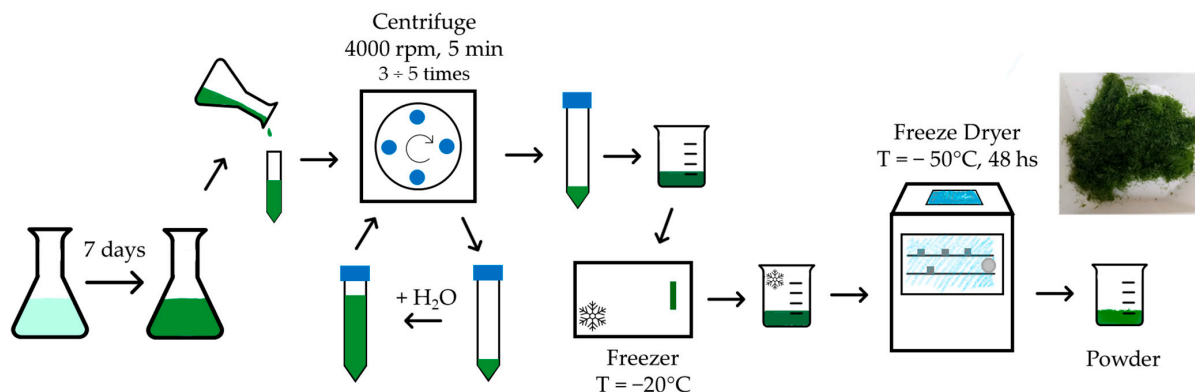


Figure 1. Dried microalga preparation scheme.

2.3. Biosorption Procedure

2.3.1. Dried Cells

First, biosorption from single-ion solutions were performed. Stock metal solutions of 1 mg/mL stored at room temperature (20 ± 1 °C) were used to reach the desired concentration of metal in the contacting aqueous solution. After adjusting the pH of the metal solutions to pH 6 and pH 7 (Hanna Instrument HI 221 pH Meter, Woonsocket, RI, USA) by means of NaOH (1 M) and HCl (1 M), the biosorption of Pb(II), Cd(II), and Cr(III) ions, respectively, 0.5 mg/L, 0.2 mg/L, 0.2 mg/L (data coming from BATs reference documents of different productive sectors: ceramic manufacturing, ferrous metals processing, and surface treatment of metals and plastics [46–48]), was carried out by contacting the solution with the microalgal biomass (0.3 g/L corresponding to $5 \times 10^9 \pm 1 \times 10^9$ cells/L). Throughout all the experiments, the pH remained constant at the fixed initial pH, with a maximum variation of ± 0.5 . After the reaction time of 2 days, samples of 10 mL of solution were taken and filtered by syringe filters of 0.22 μm pore diameter (Rotilabo[®], Karlsruhe, Germany) to remove all the cells. The filtrate was analysed with ICP-OES (Spectro Ametek, Spectro Analytical Instruments GmbH, Kleve, Germany), to determine the residual metal concentration. The remaining solution was centrifuged, to recover the biomass, or, when necessary, it was kept continuing the experiment. Centrifugation was performed at 4000 rpm for 5 min, followed by washing with MilliQ 3 to 5 times. Then, the recovered algae were frozen at -20 °C for a few hours and then freeze-dried at -50 °C for 48 h to obtain metal-loaded algal biomass (Figure 2). Also, multi-ion experiments were carried out, maintaining the same initial concentrations and operative conditions as the single-ion adsorption experiments: 0.5 mg/L of Pb(II), plus 0.2 mg/L of Cr(III), plus 0.2 mg/L of Cd(II), for a total heavy metals amount of 0.9 mg/L.

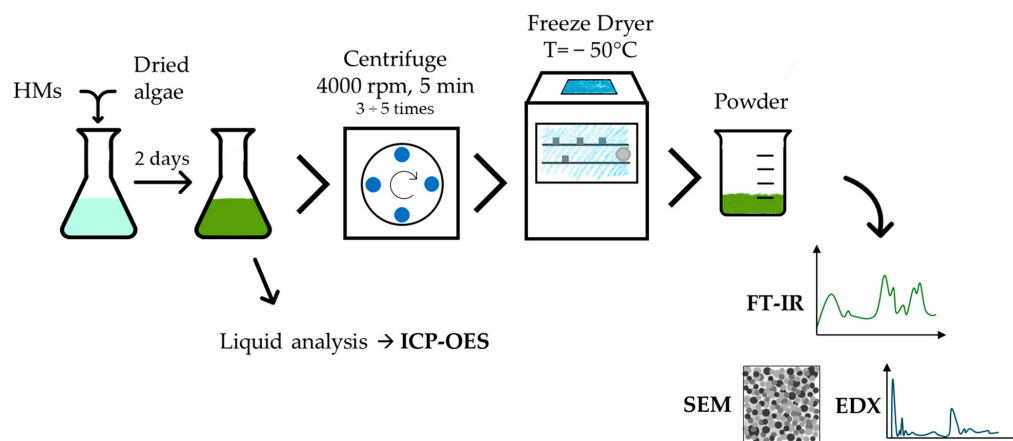


Figure 2. Biosorption procedure and samples (powder) preparation.

2.3.2. Living Cells

After that, experiments with living *C. reinhardtii* were conducted. The stock culture of the algae was maintained in Kuhl medium (Table S3). For the experiment, a portion of the microalgae were taken off the medium and washed 5 times with MilliQ water to remove any residue of the medium. Then, the still living cells (determined by their moving) were added to Cd(II) solution to reach a concentration of 0.2 mg/L, as done for the dried cells. The cell concentration was $5 \times 10^9 \pm 1 \times 10^9$ cells/L (same as for the dried cells), and the pH was kept at pH 6. The algae were further cultured at room temperature ± 20 °C and at 12 h/12 h LED illumination. After 2 and 4 days, samples of 10 mL of solution were taken off the experimental flask and filtered by syringe filters of 0.22 μm pore diameter (Rotilabo[®], Karlsruhe, Germany). The filtrate was analysed with ICP-OES (Spectro Ametek, Spectro Analytical Instruments GmbH, Kleve, Germany), to determine the remaining Cd(II) concentration and calculate the adsorption to living cells. The still living cells were harvested after 2 and 4 days, frozen at -20 °C for a few hours, and then freeze-dried at -50 °C for 48 h. The freeze-dried cells were further analysed by FTIR-ATR and SEM-EDX.

2.4. Materials Characterization

Liquid solutions were analysed before and after algae treatment by ICP-OES, to understand their chemical composition and to investigate the biosorption of the HMs by microalgae.

Chemical speciation in solution as a function of pH was calculated a priori by means of the Hydra-Medusa software v0.1.1 [50], which contains a database with logK data at 25 °C. Running the program, it is possible to obtain information on ionic species at the equilibrium as a function of a selected parameter, in this case, pH.

C. reinhardtii was characterized by different characterization techniques before and after the adsorption of metals. Zeta potential (ZP)–Zero Point Charge (ZPC) was determined by a Zetasizer Nano ZS (Malvern Instruments Limited, Malvern, UK). Dynamic Light Scattering (DLS) at 90°, with a Non-Invasive Backscatter (NIBS) optics was used for the measurements. The measurement was performed on a concentration of microalgae of 5 g/L, at the pH of the algae in water (pH 6.5). Fourier-Transform InfraRed (FT-IR) spectroscopy was used to analyse the functional groups of the pristine microalga and their interaction with heavy metals when adsorbed. Samples were analysed using a Thermo Nicolet Nexus equipped with Smart iTX accessory (Thermo Fisher Scientific, Waltham, MA, USA), diamond window, (ATR technique) and OMNIC acquisition software v7.2, with 100 scans and 4 cm^{-1} of resolution. Scanning Electron Microscopy (SEM) analysis was performed for the *C. reinhardtii* surface before and after being contacted with metals. Analyses were performed with a Zeiss EVO 50 EP (Zeiss, Jena, Germany) combined with Oxford INCA energy 2000 spectrometer (Oxford Instruments, Abingdon, UK). The SEM-EDX equipment was operated at an electron high tension (EHT) voltage of 15 and 20 kV, a probe current of 120 and 300 pA, and at high vacuum (about 10^{-4} Pa) conditions. Before the analysis, the samples were gold coated (layer thickness: 10 nm) with an Edwards Sputter Coater S150B (Edwards, Crawley, UK) to provide conductivity to the sample and to avoid electrostatic overcharge.

3. Results

3.1. Biosorbent Characterization

Dried *C. reinhardtii* was fully characterized by different techniques. Upon drying, the surface of the microalga was characterized by a negative ZP of -18.8 mV.

A FTIR (ATR mode) full spectrum of the dried biomass is plotted in Figure 3 and the low frequency region is magnified in Figure S1. Additionally, for clarity, the characteristic bands found by FT-IR analysis and their assignation are summarized in Table S4.

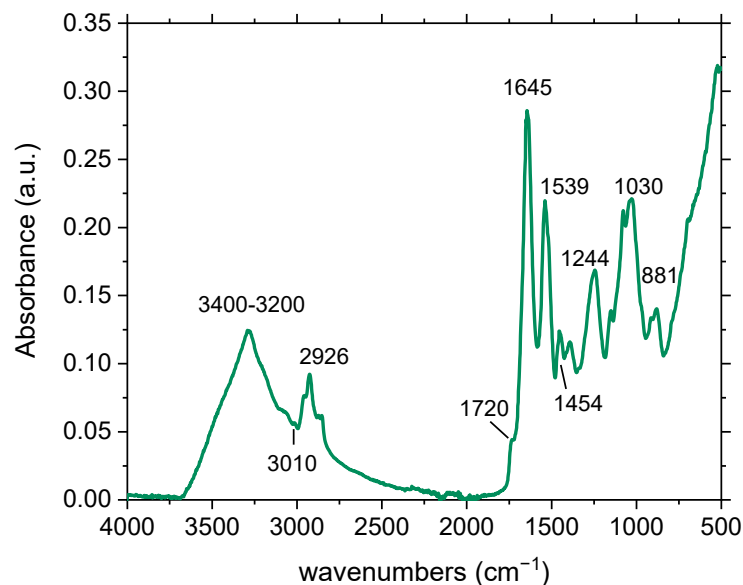


Figure 3. FTIR in ATR mode spectrum of pristine *C. reinhardtii*.

Analysing the spectrum, different regions can be identified.

The first is region I (4000–2000 cm^{-1}) (Figure 3). In the high frequency region of the spectrum, a broad and complex band at 3400–3200 cm^{-1} , centred around 3290 cm^{-1} , is visible due to the overlapping of the -OH and -NH functional groups' stretching modes [35,36,42]. The band broadness is typical of the H bonding interaction of the OH groups. The complex bands located around 2955–2855 cm^{-1} are assigned to the CH stretching modes [35,36,42] while the very small band at 3010 cm^{-1} is assigned to the unsaturated =C-H stretching [36].

The second is region II (2000–1000 cm^{-1}) (Figure 3 and Figure S1). In the medium frequency region of the spectrum, the main bands are centred at 1645 cm^{-1} and 1539 cm^{-1} , and they can be assigned to the amide I and amide II bands of the peptide linkage in proteins. The former band is associated mainly with C=O stretching vibration, while the latter band mainly with a combination of N-H in plane bending and CN stretching vibration [35,42,51,52]. The amide III component falls between 1320–1230 cm^{-1} , thus partially overlapping with other vibrational modes as discussed in the following. A shoulder at 1720 cm^{-1} can be related to C=O stretching bonds in carboxylic groups or, more likely, in ester groups in acylglycerols, and thus in the lipid fraction of the biomass [36,51,52]. The complex band at 1454 cm^{-1} represents the CH₂ and CH₃ bending [35,52], while the band at 1244 cm^{-1} can be assigned to the phosphate P=O group and to the OCO vibrational mode of the ester group [36,52].

The third is region III (1000–500 cm^{-1}) (Figure 3 and Figure S1). Here, the complex envelope of bands with several maxima at 1030/1000 cm^{-1} is due to C-O and C-C stretching modes of the polysaccharide fraction [35,36]. The bands near 881 cm^{-1} refer to out-of-plane OH bending. Thus, the FT-IR spectrum of dried *C. reinhardtii* matches those found in the literature where the alga cell wall has been described as a “multi-layered wall” consisting of hydroxyproline-rich molecules, glycosidically linked to galactose (mainly) and to arabinose [53,54].

The morphology of the dried *C. reinhardtii* was analysed by SEM images to check possible modification of the cell wall upon drying (Figure 4b). In Figure 4a,b the typical spherical structure of CR cells is observed, along with indication of cell disruption, possibly due to the freeze-drying process.

In the literature it is reported for *Chlorella vulgaris* that signs of pitting and damage on the cell wall, distortion, and collapse are consistent with the drying process [55]. Therefore, similar effects can be inferred regarding pristine *C. reinhardtii* upon freeze drying, as clearly shown by SEM picture at higher magnification (Figure 4b). To study the chemical

composition of *C. reinhardtii*, EDX analysis was also performed (Figure S2). The presence of light metals, such as K(I), Ca(II), and Mg(II), and an intense phosphorous (P) peak could be identified. These essential elements are present in all cells and supplied by the growth medium (Table S3) [52].

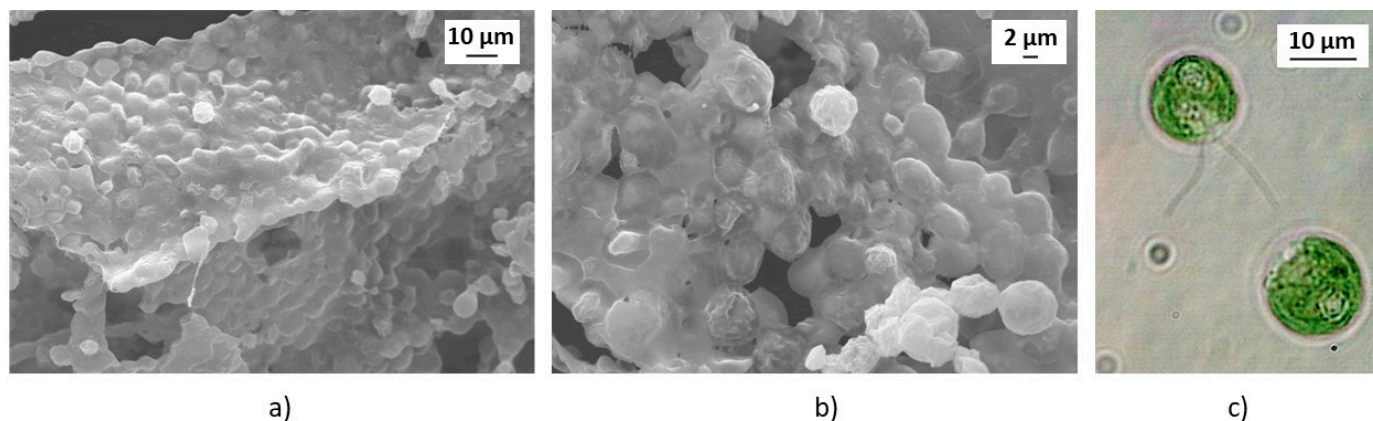


Figure 4. Scanning Electron Microscopy (SEM) pictures of pristine dried *C. reinhardtii* at different magnifications: (a) 2.50 KX and (b) 5.00 KX. (c) Optical microscope image of the living algae.

3.2. Biosorption on Dried Algae

3.2.1. Single-Ion Solutions

The adsorption process of Pb(II), Cr(III), Cd(II) to dried *C. reinhardtii* was studied by contacting the dried microalgae with single-ion solution at a fixed initial concentration, namely 0.5 mg/L for Pb(II), 0.2 mg/L for Cr(III), and 0.2 mg/L for Cd(II). Experiments were performed at two different contact times, 2 and 4 days, and two operating pH, i.e., 6 and 7. The remaining concentration of these metals after the contact time was recorded by ICP-OES. Results of ICP-OES on the supernatant solution after centrifugation are plotted in Figure 5a,b, and summarised in terms of absolute values in Table S5.

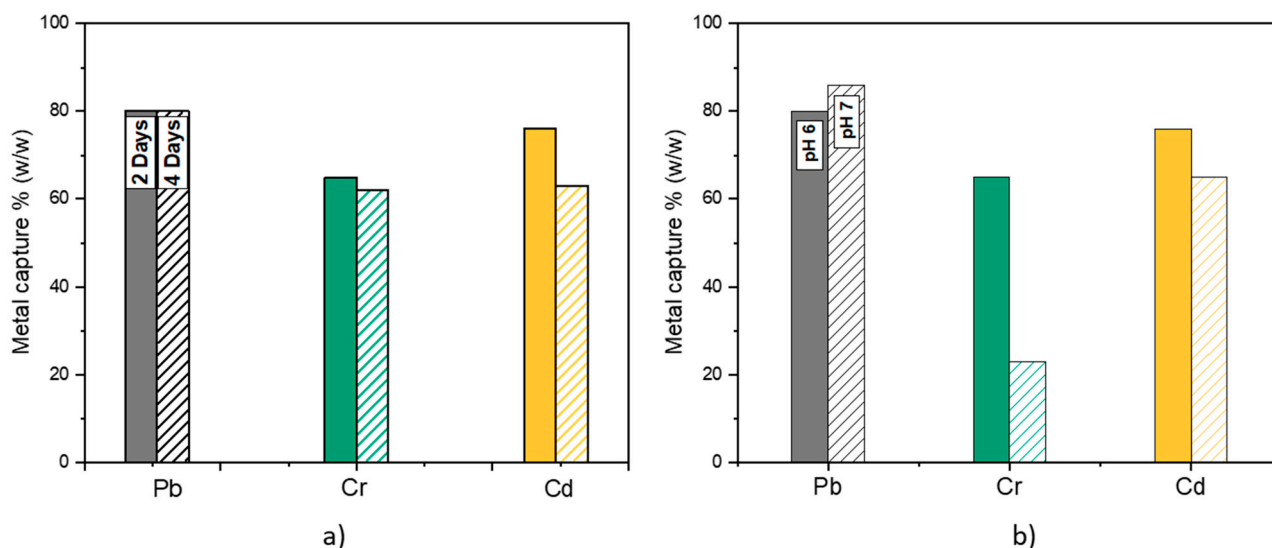


Figure 5. Effect of (a) contact time, and (b) solution pH in single-ion metal solution.

Adsorption of about 80% (*w/w*) for Pb(II) and Cd(II), and 65% (*w/w*) for Cr(III) were reached after 2 days of contact time (Figure 5a). A longer contact time of 4 days does not enhance the biosorption, and it gets worse in case of Cr and Cd ions. Accordingly, 2 days was considered as the correct contact time and it was applied to all further experiments. The effect of the operating pH was studied by varying pH through the addition of NaOH (1 M) or HCl (1 M). The solution pH was fixed at the required value at the beginning and

then it was monitored throughout the experiment. Maximum pH variation during the contact time was ± 0.5 ; hence, no further pH correction was required. It is evident that by operating at pH 6, a larger amount of Pb and Cr ions were captured by the microalgae, while no or negligible pH effect occurred in the case of Cd solution (Figure 5b). Accordingly, pH 6 was adopted for further experiments.

After the adsorption process, the algae were dried and further characterized. FTIR spectrum of *C. reinhardtii* after metal adsorption at pH 6 is plotted in Figure 6; here, the spectrum of the pristine alga is reported for comparison (full spectra of the microalga before and after adsorption at pH 6 can be found in Figure S3). The biomass structure is not heavily affected by metal adsorption, given that the positions of the main FTIR bands of the exhausted *C. reinhardtii* are close to those detected in the pristine microalga (Figure S3). However, small differences common to all the spectra of the used biomass, regardless the adsorbed metal ion, can be noticed. First, the main and broad band, centred at 3291 cm^{-1} , is reduced in intensity, the small band at 3010 cm^{-1} , associated to the =C-H stretching mode disappears. Also, a slight modification of the complex band at $2955\text{--}2855\text{ cm}^{-1}$ is evident. In Figure 6, the shoulder around 1720 cm^{-1} almost disappears, and the band at 1244 cm^{-1} is strongly reduced in intensity, as well as the band at 881 cm^{-1} . Some variations are also detectable in the region of CO/CC stretching around $1030\text{--}1000\text{ cm}^{-1}$, characterising the carbohydrate component, whose bands are more defined after adsorption.

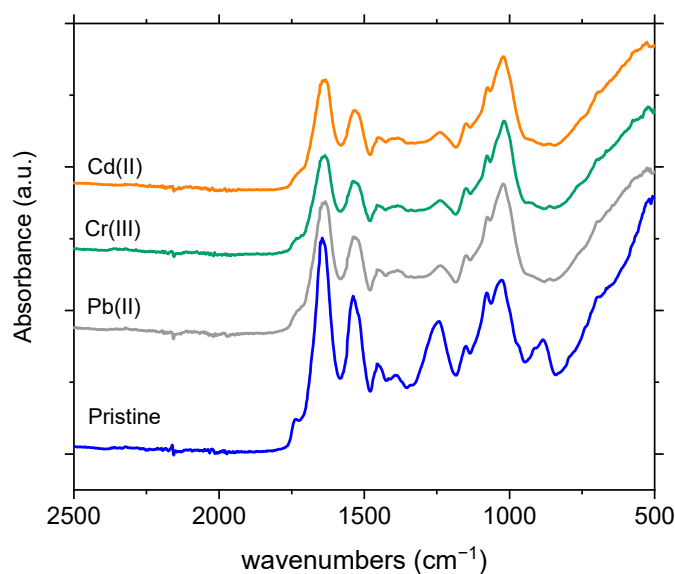


Figure 6. FTIR-ATR spectra of the alga before (pristine alga) and after the adsorption of the HMs at pH 6 low frequency region.

SEM analysis of *C. reinhardtii* after single-metal adsorption of HMs is reported in Figure 7a,b. By comparing the images of the algae after HMs adsorption with those of the pristine one, no remarkable differences are evident, even at large magnification (Figure 7b). As already reported for the pristine alga, only the typical spherical structures of the *C. reinhardtii* cells arise, as well as the effect of the freeze-drying process effects. Indeed, signs of pitting and damage of the cell as well as distortion and collapse are clear, together with a residual number of undisrupted cells. This suggests no or limited effects of the metal on the pristine *C. reinhardtii* morphology.

In EDX analysis of Cd(II) and Cr(III) treated algae, the adsorbed ions are not visible (Figure S4), only Pb(II) is barely evident. Moreover, in EDX analysis, a small amount of metals, such as Mg(II), K(I), Ca(II), and small amount of P, already present in the pristine microalga were detected.

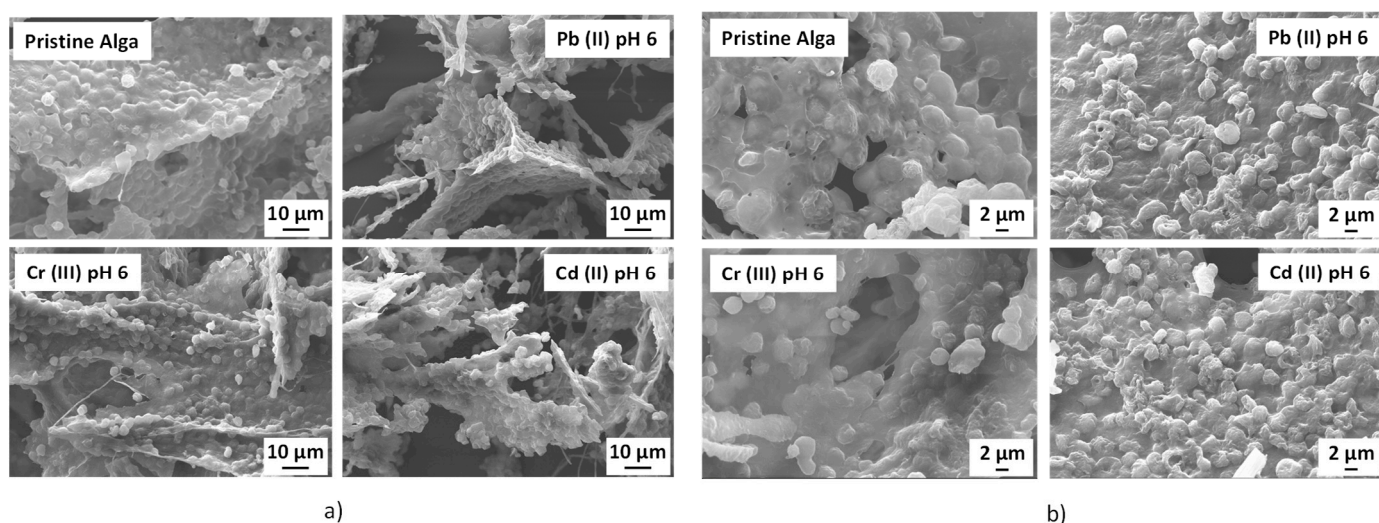


Figure 7. SEM pictures of the microalga before and after metal adsorption in single-ion solutions at pH 6 at different magnifications: (a) 2.50 KX and (b) 5.00 KX (5.21 KX for Cr).

3.2.2. Multi-Ion Solutions

Wastewater streams are complex solutions containing different pollutants. To better study microalgae behaviour in polluted water streams, and their ability to remove HMs, multi-ion systems maintaining the previous concentrations were studied.

In Figure 8, metal capture by dried cells in multi-ion solution at pH 6 is reported and compared with the corresponding single-ion ones, while quantitative results are reported in Table S6. In multi-ion solution, the removal of Pb(II) and Cr(III) increased, respectively, from 80% (*w/w*) to 91% (*w/w*) and from 65% (*w/w*) to 85% (*w/w*), while the capture of Cd ions decreased from 76% (*w/w*) down to 59% (*w/w*), suggesting a possible competition effect.

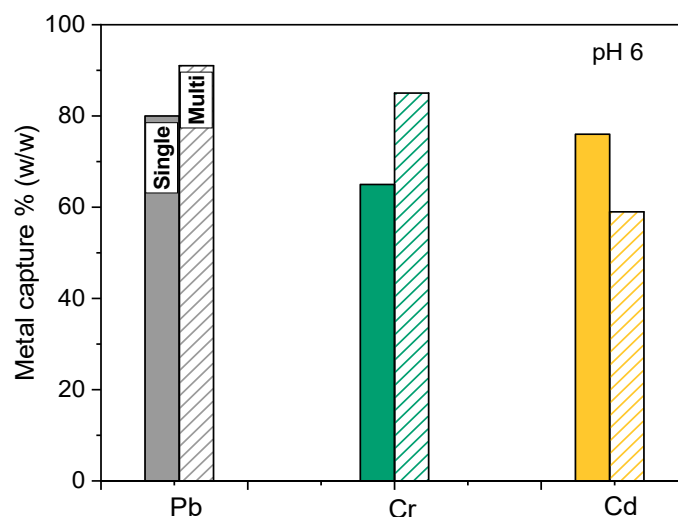


Figure 8. Comparison of metal capture in multi- and single-ions solutions.

Results of metal capture in $\mu\text{mol}_{\text{ion}}/\text{g}_{\text{microalgae}}$ in both single- and multi-ion solutions are plotted in Figure 9 and reported in Table S7. The overall absolute capture behaviour of the microalga follows the same trend in both systems: Cr(III) > Pb(II) > Cd(II). However, the multi-metal system pictures a total increase in captured moles; in particular, Pb(II) adsorption increases by 0.8 μmoles , and Cr(III) by 2.5 μmoles , while Cd capture decreases by 1 μmole . The decrease of Cd(II) adsorption (1 $\mu\text{mol}_{\text{tot}}/\text{g}_{\text{microalgae}}$) does not account for the total increase of Pb(II) and Cr(III) (3.3 $\mu\text{mol}_{\text{tot}}/\text{g}_{\text{microalgae}}$).

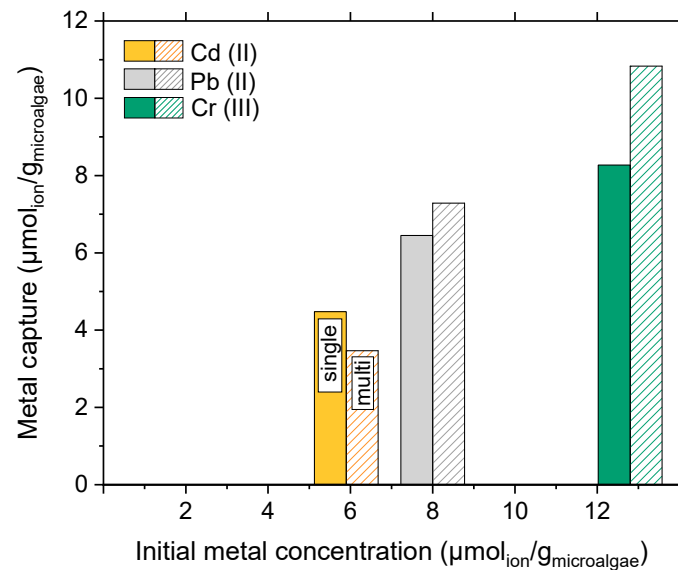


Figure 9. Metal capture in $\mu\text{mol}_{\text{ion}}/\text{g}_{\text{microalgae}}$ in both single- and multi-ion solutions.

Also, the effects of metal-treated algae upon adsorption experiments in multi-ion solutions were fully characterized. In Figure 10, FT-IR spectra of the pristine alga before and after metal adsorption in multi-ion systems are plotted.

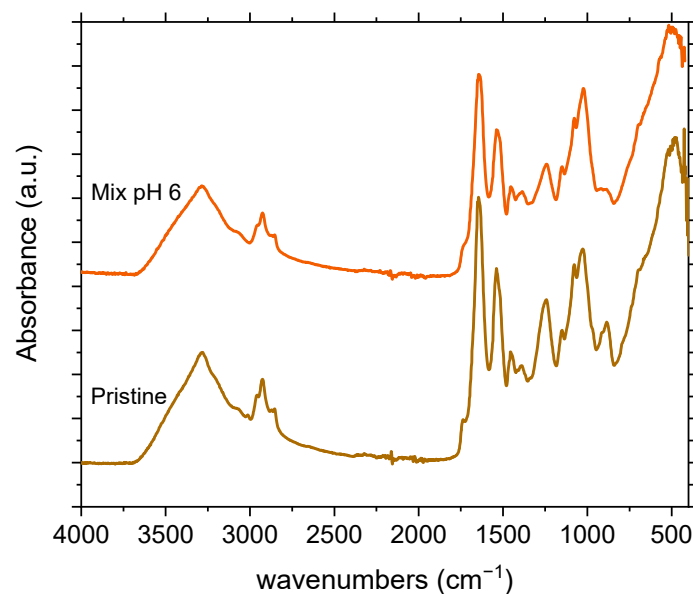


Figure 10. FTIR-ATR spectra of the alga before and after metal adsorption in multi-ion systems.

No marked differences were found when spectra of the treated algae were compared with those of the pristine one (Figure 10). A broadening of the main band, centred at 3291 cm^{-1} , occurred, as well as of the complex band at $2955\text{--}2855\text{ cm}^{-1}$. Broadening is also observed for the shoulder around 1720 cm^{-1} , while the band at 1244 cm^{-1} is reduced in intensity. However, the most remarkable difference between mono- and multi-ion systems regards the region around 900 cm^{-1} , where the out-of-plan bending of the OH groups is still visible. This band completely disappeared upon the adsorption of metal ions in all single-ion solutions, while it is still weakly visible in the plot of multi-ion solution (Figure 10). This result suggests that, upon contacting the bio-sorbent with the multi-ion system, a different interaction of the metals with OH functional groups are active. Thus, a possible different adsorbate–sorbent interaction is possible, related to the modification

of the binding sites and/or different ionic species to be adsorbed. However, this point, considering the system complexity, deserves further studies to be confirmed.

In Figure 11, SEM micrographs of the alga before and after the metal capture in multi-ionic solution are reported at two different magnifications and compared with those of the pristine alga.

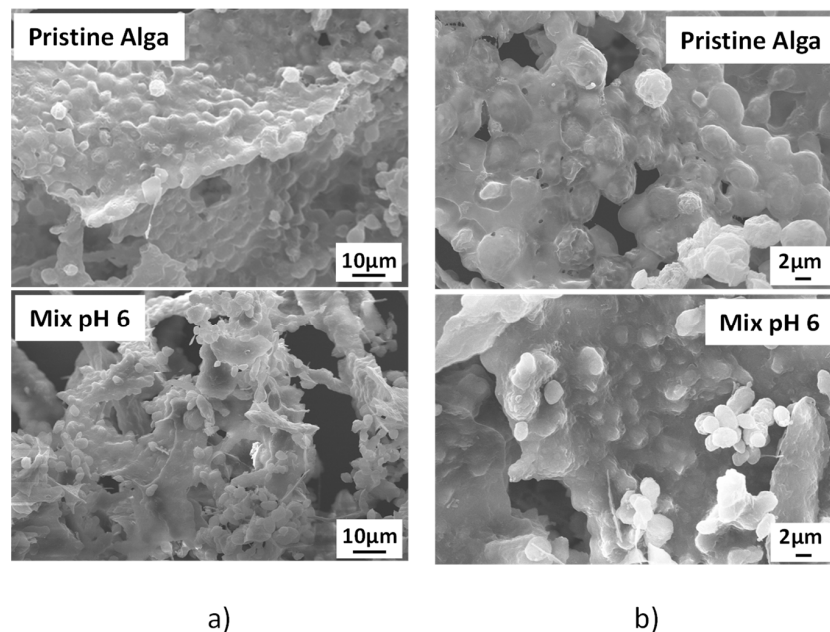


Figure 11. SEM pictures of the microalga before and after metal adsorption in multi-ion solutions at different pH magnifications: (a) 2.50 KX and (b) 5.00 KX.

Also, in this case, only the effect of cell drying, such as pitting, cell damage, distortion and collapse, is observable [55], with no evidence of the algae–metal interaction. Similarly, EDX analysis (Figure S5), did not show any evidence of Pb(II), Cr(III), and Cd(II) adsorption, and only Mg(II), K(I), and Ca(II), and P originally present in the pristine algae, were detected.

3.2.3. Preliminary Comparison of Adsorption to Living and Dried Algae: Cd(II) Case

A preliminary comparison between living and dried algae adsorption behaviour was performed on Cd solution, applying the same conditions reported above. Results of the comparison of the adsorption capacity, measured by ICP-OES of the initial and final solution of the living and the dried algae are summarized Table 1.

Table 1. Comparison between Cd adsorption in living and dried algae.

Ion	Initial Metal Concentration (mg/L)	pH	Contact Time	Dried Algae Adsorption		Living Algae Adsorption	
				mg/L	% (<i>w/w</i>)	mg/L	% (<i>w/w</i>)
Cd(II)	0.2 ± 0.002	6	2 days	0.151 ± 0.001	76	0.156 ± 0.001	78
			4 days	0.125 ± 0.001	63	0.182 ± 0.001	91

After 2 days of contact time, both living and dried algae were able to capture the same Cd amount, i.e., 78% (*w/w*) and 76% (*w/w*) of the total. However, when the contact time was prolonged for 4 days, the living algae were able to capture a larger amount of ions, up to 91% (*w/w*), while in the dried one, Cd adsorption is even lower (76% (*w/w*) and 63% (*w/w*) at 2 and 4 days of contact time, respectively).

After the contact reaction, the living cells were freeze-dried and characterized by FT-IR-ATR analysis (Figure 12).

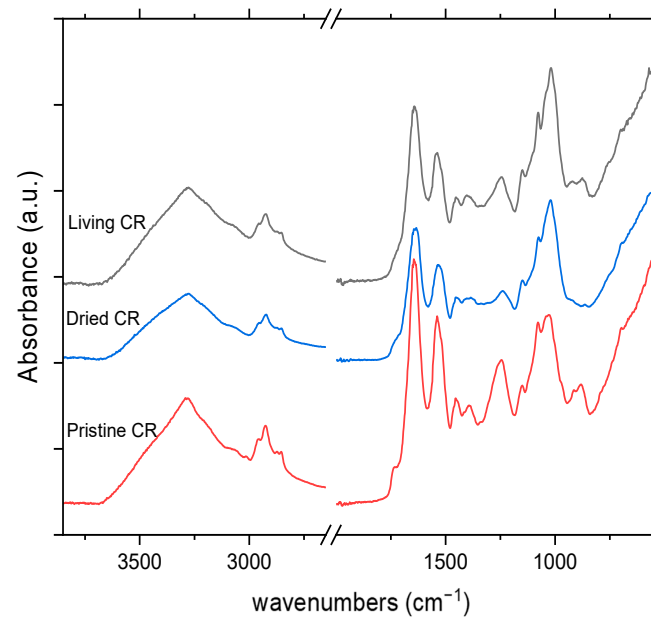


Figure 12. FTIR-ATR spectra of the living and dried algae after Cd(II) adsorption. Untreated algae spectrum is reported for comparison. Living cells were dried after being contacted with Cd solution.

No significant differences are present in the high frequency region of the living and the dried microalga after adsorption. The band centred at 1244 cm^{-1} appears to be less intense than the pristine one, but more intense than the dried microalga. Also, the low frequency region, around 800 cm^{-1} , changes following the same behaviour as before: lower intensity than the pristine, and higher intensity than the living microalga.

The morphology of the living and dried algae before and after Cd capture was analysed by SEM analysis, pictures are reported in Figure 13 at two different magnifications, namely 2.50 KX (above) and 5.00 KX (below). In dried algae (Figure 13b), only the typical effect of the drying process on the cells manifests itself. Similarly, the living algae show signs of cell wall damage [55]; however, in this sample, cells appear slightly smaller, oval-shaped, and less grouped. Also, in this case, EDX analysis (Figure S6) did not evidence any adsorption of Cd ions.

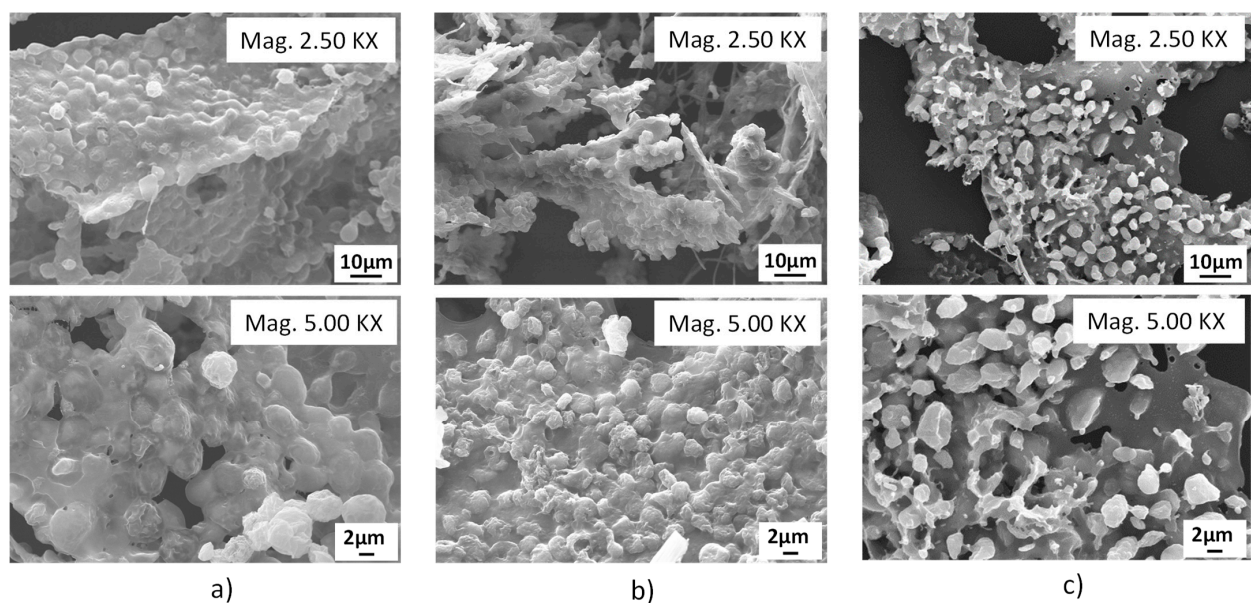


Figure 13. SEM pictures of microalga (a) before adsorption and after Cd(II) adsorption on (b) dried form and (c) living form.

4. Discussion

Heavy metals, such as Pb(II), Cr(III), and Cd(II), can be found at very low concentrations in the wastewaters of different productive sectors, e.g., ceramic manufacturing, ferrous metals processing, and surface treatment of metals and plastics [46–48]. The aim of this work is to understand the applicability of the microalga *C. reinhardtii* to treat low concentrated wastewaters (0.5 mg/L Pb(II), 0.2 mg/L Cr(III) and Cd(II)), before reintroducing them into the environment, following European regulation and limitations [49].

Despite the observed cells damage due to the applied freeze-drying process, pristine *C. reinhardtii* maintains its original metal ion adsorption capability. This result is not surprising when considering the dried biomass as a natural sorbent, consisting mainly of cellulose or proteins. Both biopolymers, are reported to be able to interact and capture metal ions [29,35,41]. The sorption capability is strictly connected to the residual functional groups present in the dried biomass as well as to the operating conditions, contact time, and pH adopted during the adsorption process.

Two days of contact were found appropriate to reach the 65–80% (*w/w*) of metal capture depending on the considered metal ion. Apparently, the algae have a larger affinity for Pb(II) and Cd(II), respectively, 80% (*w/w*) and 76% (*w/w*) of adsorption, while only 65% (*w/w*) of Cr(III) is adsorbed. However, looking at $\mu\text{mol}_{\text{ion}}$ captured by 1 g of sorbent material, it is possible to observe that Cr(III) is the most captured ion, nominally $8.3 \mu\text{mol}_{\text{Cr}}/\text{g}_{\text{microalgae}}$, while Pb(II) and Cd(II) have, respectively, been adsorbed $6.5 \mu\text{mol}_{\text{Pb}}/\text{g}_{\text{microalgae}}$ and $4.5 \mu\text{mol}_{\text{Cd}}/\text{g}_{\text{microalgae}}$. A prolonged contact time of 4 days did not influence the adsorption yields of Pb(II) and Cr(III), which remained almost constant, but it had a negative effect on Cd(II) adsorption, which decreased from 76% (*w/w*) down to 63% (*w/w*), thus from $4.5 \mu\text{mol}_{\text{Cd}}/\text{g}_{\text{microalgae}}$ to $3.7 \mu\text{mol}_{\text{Cd}}/\text{g}_{\text{microalgae}}$, suggesting a reversibility in the adsorption–desorption reaction of Cd. Similar results were reported in the literature by [10], on HMs sorption by different algal strains (*Chlorella vulgaris* and *Spirulina maxima*) studied over 10 days. By evaluating the metal removal every 2 days, the authors showed that the adsorption equilibrium was dependent on the metal type, the alga strain, and the amount of the biosorbent used in the experiment.

Regarding the observed pH effect, the affinity between the biosorbent surface and the ions species in the solution should be considered to explain the different behaviour. As a matter of fact, according to Romera et al. [56], solution pH impacts two aspects: ion solubility and biosorbent total charge, which both affect the equilibrium of the system [57,58]. Therefore, the influence of pH on the metal sorption is dependent on the functional groups of the biosorbent and on the presence of different metal species in the solution, thus governing the adsorption behaviour [59,60]. To reach a deeper insight, chemical speciation in solution was calculated as a function of pH by means of the Hydra-Medusa software [50], the plots for the single-ion system are reported in Figure S7a–c. As a general consideration, at every pH, positive charged or neutral metal species are present; therefore, the interaction with the negative charged surface of the dried alga is favoured. Considering the complexity of the equilibria and species distribution of Figure S7a–c, in Figure 6 the possible main ion species present at pH 6 and 7 are summarized.

At pH 6, the Pb ion is present in the stable form of Pb^{2+} , and in a negligible amount in the form of PbOH^+ . The main species in solution of Cr-containing system are Cr_2O_3 and CrOH^{2+} , accompanied by a limited amount of $\text{Cr}(\text{OH})_2^+$ and $\text{Cr}(\text{OH})_3$. Cd metal, instead, is always present as Cd^{2+} . At pH 7, the presence of Pb^{2+} , PbOH^+ , Cd^{2+} , and Cr_2O_3 is confirmed, while all the other species are negligible.

The constant and high capture of lead can be explained by the interaction of charges of opposite sign; the simple positive ion species Pb^{2+} easily interacts with the negative surface of the bio-sorbent ($\text{ZP} = -18.8 \text{ mV}$). On the contrary, the decrease of chromium adsorption, observed for increasing pH, can be related to the progressive formation of neutral species, i.e., Cr_2O_3 , which are able to interact with the sorbent in a weaker way (e.g., Van Der Waals interaction) than the charged ones, i.e., CrOH^{2+} , present at pH 6. It is not surprising that a lower Cr adsorption is detected at pH 7, where the progressive increase of neutral species

formation occurs at the expense of the charged $\text{Cr}(\text{OH})_2^+$ and CrOH^{2+} . Moreover, Cr(III) adsorption at pH 7 could be affected by a higher steric hindrance of the Cr species, despite charged one, thus preventing higher metal capture. This is different to the case of Cd(II), where pH effect on the adsorption is not explained by charge interaction. Indeed, Cd ions are always present as Cd^{2+} , and the formation of low amount of neutral species, as reported by [61], is not able to fully explain the observed marked adsorption decrease from pH 6 to pH 7 (from 76% (*w/w*) down to 65% (*w/w*)). It can be hypothesized that charged species at different pH are characterized by different water molecules' coordination spheres which imply a larger steric hindrance at pH 7, hence a decreased availability of the adsorption sites. As a matter of fact, more sterically encumbered species cover larger surface portions and/or suffer for repulsions due to overlapping of the coordination sphere.

The nature and the extent of the coordination sphere of the different ions can be explained by considering ionic radii and charge density. Indeed, Pb(II) ions are reported to be weakly hydrated because of their low charge density. Pb(II) compounds normally crystallize without water coordination and thereby are unable to form a complete hydration shell [62]. On the contrary, complexes with high coordination number are reported for Cd ions, such as $\text{Cd}_2^+(\text{H}_2\text{O})_6(\text{H}_2\text{O})$ [63]. Accordingly, the resulting steric hindrance can be accounted to explain the difference in metal capture, mainly at higher pH. Furthermore, considering this algal biomass, a correlation has been proposed between the ionic radii of the metal cations and the affinity of the biosorbent; the larger the ionic radius the stronger the affinity [37]. Considering the ionic radii ranking, Pb^{2+} (1.32 Å) > Cd^{2+} (1.03 Å) > Cr^{3+} (0.65 Å) [64], a preferential biosorption of Pb ions, followed by Cd and Cr, may occur.

According to the performed characterization studies, an electrostatic interaction between the metals and some microalgal functional groups, i.e., amino, hydroxyl, acylglycerol, and phosphate groups, is suggested by FT-IR analysis. Indeed, these are electron-rich groups that are able to interact with the positively charged cations consistently with the negative ZP measured, and the process conditions do not affect their availability to the adsorption phenomena. The EDX results show a decrease of the peak-intensity of the light metals (i.e., Mg(II), K(I), and Ca(II)) naturally present in the pristine alga upon Pb, Cr, and Cd solution, suggesting an ion-exchange mechanism between those ions already present on the cell surface and those of interest. The absence of Cr(III) peak EDX spectra can be related to the very low metal amount used and to the overlapping of detection regions [65].

Considering the evidence of (1) experimental data, the (2) nature of the species in solution, the (3) effect of steric hindrance, and (4) ionic radii, the affinity ranking $\text{Pb} > \text{Cd} > \text{Cr}$ is considered highly plausible in case of the use of *C. reinhardtii* as biosorbent in our conditions.

The comparison between the microalgal adsorption at pH 6 in single-metal systems and in multi-metal systems is reported in terms of captured $\mu\text{mol}_{\text{ion}}/\text{g}_{\text{sorbent}}$ in Table S7, to correctly compare the behaviour of the alga toward a complex matrix. The overall absolute capture behaviour of the microalga follows the same trend in both systems: $\text{Cr}(\text{III}) > \text{Pb}(\text{II}) > \text{Cd}(\text{II})$. However, the multi-metal system displays a total increase in captured moles, in particular, Pb adsorption increases of 0.8 μmole , Cr of 2.5 μmoles , and Cd capture decreases of 1 μmole .

Ionic species distribution in single- and multi-ion solutions, calculated by Hydra-Medusa, reported in Figure S8, are compared in Table 2. As can be observed, the main species arising are the same both in the single-ion system and in multi-ion systems.

4.1. Pb(II) and Cd(II) Ions in Multi-Ion Systems

At first glance, in multi-ion systems at the studied operating conditions (reported at Section 2.3), Pb(II) and Cd(II) adsorption seem to be subjected to site competition. Similarly to single-ion systems, the difference of capture between Pb(II), showing a higher adsorption, and Cd(II), showing a lower adsorption, can be related to the nature and to the charge density of the ions. Pb(II) has a lower charge density and a higher ionic radius. Cd(II) forms highly coordinated complexes, implying a low availability of the adsorption sites,

and has a small ionic radius. According to the discussion on single-ion adsorption, a lower charge density is related to a smaller extent of the coordination sphere, and a higher radius is related to a higher affinity. In these terms, they display a respective increase and decrease of adsorption of 1 μmol . With both ions being bivalent, a site competition is proposed.

Table 2. Main ionic species by Hydra-Medusa calculation and corresponding ionic strength (single-ions reported for comparison).

Metal Ion	Single-Metal		Multi-Metals	
	Species	Ionic Strength	Species	Ionic Strength
Pb(II)	Pb ²⁺ PbOH ⁺	7.23	Pb ²⁺ PbOH ⁺	
Cr(III)	CrOH ²⁺ Cr ₂ O ₃	20.22	CrOH ²⁺ Cr ₂ O ₃	32.75
Cd(II)	Cd ²⁺	5.34	Cd ²⁺	

4.2. Cr(III) Ions in Multi-Ion Systems

At the studied operating conditions, the multi-ion system shows a strong increase in Cr(III) adsorption. Cr(III) is trivalent, in this sense its adsorption sites may be different from the bivalent ions and it will not be subjected to site competition. By considering the initial concentration in $\mu\text{mol}_{\text{ion}}/\text{g}_{\text{microalgae}}$, the higher the particle concentration, the higher the probability of collision, thus the higher the aggregation rate [66]. The ionic strength of the multi-ionic system is higher than those of single metal solutions (Table 2), this influences the precipitation of the species. Moreover, the higher the ionic strength, under certain concentrations (0.15 M reported by [67]), the higher the aggregation probability and thus, the higher the precipitation. Therefore, in these specific operating conditions, chromium capture increase can be related to aggregation and precipitation reasons, rather than adsorption itself.

Also, in this case, FT-IR analysis suggests an electrostatic interaction between the metal cations and the electron-rich microalgal functional groups. Although it is not possible to clearly evaluate a preferential interaction of the different cations with specific groups, it is possible that in multi-metal experiments, hydroxyl groups are more affected by the adsorption process than in single-metal adsorption. This should be due to the higher total amount of metal ions in solution. Concerning SEM analysis, the co-presence of the three ions has no or limited effects on the microalga morphology. The absence of representative peaks in EDX analysis must be considered as related to the very low concentration under study.

4.3. Adsorption to Living and Dried Algae: Cd(II) Case

In this experiment, living microalgae were treated with Cd for 4 days. After 2 and 4 days, the remaining concentration of Cd in the solution was investigated and the Cd adsorption to the microalga was calculated. After the experiment, i.e., after 2 or 4 days, the algae were freeze-dried and further analysed. Up to two days, Cd adsorption appears to be almost the same for both dried microalga and living microalga. However, by continuing the experiment for another two days, a decrease in adsorption is visible for dried algae, while an increase occurs in living microalgae. This difference highlights the reversibility of the adsorption process to dried microorganisms and the stability in living microalgae, probably due to bioaccumulation inside the alga itself. By bioaccumulation, the living microalgae take up the metals' ions and store them inside the cells. In living cells, two mechanisms of uptake of metal ions occur: first biosorption, i.e., the adsorption of metals ions onto the cell surface due to negatively charged functional groups and secondly, bioaccumulation, by which the metals are transported into and stored inside the cells.

FT-IR spectra show the same trend both in living and dried sorbent, with a slightly higher intensity in two regions: 1244 cm^{-1} and 1000 cm^{-1} . This can be interpreted as a

lower interaction on the surface of living microalgae, due to bioaccumulation inside the cell, contrary to what happens to dried microalgal surface.

SEM images of living adsorbent show smaller, oval-shaped, and less-grouped cells.

5. Conclusions and Future Developments

Microalgal adsorption represents a sustainable solution for the removal of heavy metals from polluted water streams. The biomass of dried *C. reinhardtii* is able to capture Pb, Cr, and Cd from water solution, even when in low concentration, showing a high efficiency removal up to 80–90% (*w/w*). The capture process is governed by the negatively charged surface wall of the dried *C. reinhardtii*, which can electrostatically bind the positively charged ions, and weakly (e.g., Van der Waals interactions) bind the neutral species. The exposed electron-rich functional groups of the algae cell wall are involved in the interaction with cations through coordination and electrostatic interactions. pH has a strong influence on the distribution of the species that can actively take part in the adsorption process; however, it apparently does not directly affect the algal functional groups at the surface of the cell wall. *C. reinhardtii* metal affinity depends on the nature of the ionic species, on steric hinderance, and on ionic radii. The affinity ranking proposed is $Pb > Cd > Cr$ for multi-ion solutions. Considering multi-metal solutions, a site competition for Pb and Cd is proposed since they are both bivalent and show a strong difference in charge density and in ionic radius. SEM analysis of the alga before and after metal adsorption showed the disruption, damage, distortion, and collapse of the spherical cell typical of the drying process, while no evidence of an additional effect of the metal capture was found. First experiments show that the HM removal capacity of living algae is even higher than that of dried biomass, probably due to additional bioaccumulation inside the cells.

The performed study is particularly useful for wastewater treatments under low metal concentration solutions. In future papers, the investigation should be performed under increased equimolar concentration to better study the sorbent, its affinity, and its selectivity ranking.

Supplementary Materials: The following supporting information can be downloaded at: <https://www.mdpi.com/article/10.3390/app142311057/s1>, Figure S1: FTIR in ATR mode low frequency region spectrum of pristine *C. reinhardtii*; Figure S2: EDX analysis of pristine dried *C. reinhardtii*. Au* peak is related to gold plating of samples to make them conductive; Figure S3: FTIR in ATR mode of the microalga before (namely, pristine) and after the adsorption of the HMs at pH 6 full spectra; Figure S4: EDX analysis of the microalga after single metal adsorption at pH 6; Figure S5: EDX analysis of the microalga after multi-metal adsorption at pH 6. Au* peak is related to gold plating of samples to make them conductive; Figure S6: EDX analysis of the living microalga after Cd adsorption. Au* peak is related to gold plating of samples to make them conductive; Figure S7: Hydra-Medusa plots for: (a) Pb(II), (b) Cr(III), and (c) Cd(II) single-ion solution; Figure S8: Hydra-Medusa plots of the multi-ionic solution; Table S1: capture of metal ions using living and dead biomass; Table S2: Metal concentration of industrial wastewater streams (BAT reference documents); Table S3: Kuhl Medium composition for the algae growth; Table S4: Characteristics IR bands and functional groups detected in the samples; Table S5: Dried algae metal adsorption at different contact times at pH 6; Table S6: Nominal results of dried algae metal adsorption at pH 6 in single and in multi-ion solutions; Table S7: nominal results ($\mu\text{mol}_{\text{ion}}/\text{g}_{\text{algae}}$) of dried algae metal adsorption at pH 6 in single and in multi-ion solutions after 2 days of contact time. References [10,35–39,41,42,46–48,51,52] are cited in the supplementary materials.

Author Contributions: Conceptualization, G.S.; methodology, M.G.G., G.S., and C.C.; software, M.G.G.; formal analysis, M.G.G. and M.G.; investigation, M.G.G., M.G., E.F., and C.C.; resources, C.C., G.S., and G.D.; data curation, M.G.G., G.S., and C.C.; writing—original draft preparation, M.G.G.; writing—review and editing, M.G., C.C., G.S., and E.F.; visualization, M.G.G., M.G., and C.C.; supervision, G.S. and C.C.; project administration, G.S.; funding acquisition, G.S. All authors have read and agreed to the published version of the manuscript.

Funding: G.S. was funded by the German Federal Ministry for Economic Affairs and Climate Protection (BMWK) in the frame of ZIM program (HybridFilter). Funding number: KK5244302MR2.

Institutional Review Board Statement: Not applicable.

Informed Consent Statement: Not applicable.

Data Availability Statement: The data are contained within the article.

Acknowledgments: Thanks are given to Mattia Ronchi and Cinzia Ferrario (SAMM Lab, Politecnico di Milano, Dipartimento di Chimica, Materiali e Ingegneria Chimica “Giulio Natta”) for their help in performing Scanning Electron Microscopy equipped with Energy Dispersive X-ray analysis (SEM-EDX), to Gilberto Artioli (Padova University) for the determination of the ZP, and to Samir Hammoud (MPI-IS, Stuttgart) for performing ICP-OES analysis. Part of this work was carried out during a master thesis project carried out by M.G.G. at the University of Stuttgart, Germany under the Erasmus+ program.

Conflicts of Interest: The authors declare no conflicts of interest. The funders had no role in the design of the study, in the collection, analyses, or interpretation of data, in the writing of the manuscript, or in the decision to publish the results.

References

1. Govind, P. Heavy Metals Causing Toxicity in Animals and Fishes. *Res. J. Anim. Vet. Fish. Sci.* **2014**, *2*, 17–23.
2. Dai, S.; Graham, I.T.; Ward, C.R. A Review of Anomalous Rare Earth Elements and Yttrium in Coal. *Int. J. Coal Geol.* **2016**, *159*, 82–95. [[CrossRef](#)]
3. Pinotti, L.; Ottoboni, M.; Giromini, C.; Dell’Orto, V.; Cheli, F. Mycotoxin Contamination in the EU Feed Supply Chain: A Focus on Cereal Byproducts. *Toxins* **2016**, *8*, 45. [[CrossRef](#)] [[PubMed](#)]
4. Beyersmann, D.; Koster, A.; Buttner, B.; Flessel, P. Model Reactions of Chromium Compounds with Mammalian and Bacterial Cells†. *Toxicol. Environ. Chem.* **1984**, *8*, 279–286. [[CrossRef](#)]
5. Lester, J. *Heavy Metals in Wastewater and Sludge Treatment Processes*; CRC Press: Boca Raton, FL, USA, 1987; Volume 1.
6. Jaishankar, M.; Tseten, T.; Anbalagan, N.; Mathew, B.B.; Beeregowda, K.N. Toxicity, Mechanism and Health Effects of Some Heavy Metals. *Interdiscip. Toxicol.* **2014**, *7*, 60–72. [[CrossRef](#)]
7. Matta, G.; Gjyli, L. Mercury, Lead and Arsenic: Impact on Environment and Human Health. *JCPS* **2016**, *9*, 718–725.
8. Mandotra, S.K.; Upadhyay, A.K.; Ahluwalia, A.S. (Eds.) *Algae: Multifarious Applications for a Sustainable World*; Springer: Singapore, 2021; ISBN 9789811575174.
9. Sharma, P.; Kumar, S.; Pandey, A. Bioremediated Techniques for Remediation of Metal Pollutants Using Metagenomics Approaches: A Review. *J. Environ. Chem. Eng.* **2021**, *9*, 105684. [[CrossRef](#)]
10. Chan, A.; Salsali, H.; McBean, E. Heavy Metal Removal (Copper and Zinc) in Secondary Effluent from Wastewater Treatment Plants by Microalgae. *ACS Sustain. Chem. Eng.* **2014**, *2*, 130–137. [[CrossRef](#)]
11. Kauppila, P.; Liisa Räisänen, M.; Myllyoja, S. *Best Environmental Practices in Metal Ore Mining*; Finnish Environment Institute: Helsinki, Finland, 2011; ISBN 978-952-11-4188-1.
12. Gautam, R.K.; Sharma, S.K.; Mahiya, S.; Chattopadhyaya, M.C. Chapter 1. Contamination of Heavy Metals in Aquatic Media: Transport, Toxicity and Technologies for Remediation. In *Heavy Metals in Water*; Sharma, S., Ed.; Royal Society of Chemistry: Cambridge, UK, 2014; pp. 1–24. ISBN 978-1-84973-885-9.
13. Northey, S.A.; Mudd, G.M.; Saarivuori, E.; Wessman-Jääskeläinen, H.; Haque, N. Water Footprinting and Mining: Where Are the Limitations and Opportunities? *J. Clean. Prod.* **2016**, *135*, 1098–1116. [[CrossRef](#)]
14. Northey, S.A.; Mudd, G.M.; Werner, T.T.; Haque, N.; Yellishetty, M. Sustainable Water Management and Improved Corporate Reporting in Mining. *Water Resour. Ind.* **2019**, *21*, 100104. [[CrossRef](#)]
15. World Health Organization. Guidelines for Drinking-Water Quality: Fourth Edition Incorporating the First and Second Addenda. Available online: <https://www.who.int/publications/i/item/9789240045064> (accessed on 18 January 2024).
16. Fu, F.; Wang, Q. Removal of Heavy Metal Ions from Wastewaters: A Review. *J. Environ. Manag.* **2011**, *92*, 407–418. [[CrossRef](#)]
17. Gunatilake, S.K. Methods of Removing Heavy Metals from Industrial Wastewater. *Methods* **2015**, *1*, 14.
18. Fan, D.; Peng, Y.; He, X.; Ouyang, J.; Fu, L.; Yang, H. Recent Progress on the Adsorption of Heavy Metal Ions Pb(II) and Cu(II) from Wastewater. *Nanomaterials* **2024**, *14*, 1037. [[CrossRef](#)] [[PubMed](#)]
19. Ahmaruzzaman, M. Industrial Wastes as Low-Cost Potential Adsorbents for the Treatment of Wastewater Laden with Heavy Metals. *Adv. Colloid Interface Sci.* **2011**, *166*, 36–59. [[CrossRef](#)] [[PubMed](#)]
20. Iakovleva, E.; Sillanpää, M. The Use of Low-Cost Adsorbents for Wastewater Purification in Mining Industries. *Environ. Sci. Pollut. Res.* **2013**, *20*, 7878–7899. [[CrossRef](#)] [[PubMed](#)]
21. Giese, E.C. Biosorption as Green Technology for the Recovery and Separation of Rare Earth Elements. *World J. Microbiol. Biotechnol.* **2020**, *36*, 52. [[CrossRef](#)] [[PubMed](#)]
22. Lu, M.-M.; Gao, F.; Li, C.; Yang, H.-L. Response of Microalgae *Chlorella vulgaris* to Cr Stress and Continuous Cr Removal in a Membrane Photobioreactor. *Chemosphere* **2021**, *262*, 128422. [[CrossRef](#)] [[PubMed](#)]
23. Dirbaz, M.; Roosta, A. Adsorption, Kinetic and Thermodynamic Studies for the Biosorption of Cadmium onto Microalgae *Parachlorella* sp. *J. Environ. Chem. Eng.* **2018**, *6*, 2302–2309. [[CrossRef](#)]

24. Santomauro, G.; Sun, W.-L.; Brümmer, F.; Bill, J. Incorporation of Zinc into the Coccoliths of the Microalga *Emiliania Huxleyi*. *Biomaterials* **2016**, *29*, 225–234. [[CrossRef](#)] [[PubMed](#)]
25. Santomauro, G.; Singh, A.V.; Park, B.; Mohammadrahimi, M.; Erkoç, P.; Goering, E.; Schütz, G.; Sitti, M.; Bill, J. Incorporation of Terbium into a Microalga Leads to Magnetotactic Swimmers. *Adv. Biosys.* **2018**, *2*, 1800039. [[CrossRef](#)]
26. Santomauro, G.; Stiefel, M.; Jeurgens, L.P.H.; Bill, J. In Vivo Shaping of Inorganic Functional Devices Using Microalgae. *Adv. Biosys.* **2020**, *4*, 1900301. [[CrossRef](#)] [[PubMed](#)]
27. Pasqua, G.; Abbate, G.; Forni, C.; Acosta, A.; Baldan, B.; Basile, A.; Caporali, E.; Cozzolino, S.; Felicini, G.P.; Giovi, E.; et al. *Botanica Generale e Diversità Vegetale*, 4th ed.; Piccin: Padova, Italy, 2019; ISBN 978-88-299-2979-5.
28. Chojnacka, K.; Marquez-Rocha, F.-J. Kinetic and Stoichiometric Relationships of the Energy and Carbon Metabolism in the Culture of Microalgae. *Biotechnology* **2003**, *3*, 21–34. [[CrossRef](#)]
29. Rinanti, A.; Fachrul, M.F.; Hadisoebroto, R.; Desty, S.; Rahmadhania, R.; Widyaningrum, D.A.; Saad, N.A. Heavy metal pollutant sorption in aquatic environment by microalgae consortium. *Indones. J. Urban. Environ. Technol.* **2021**, *5*, 51–71. [[CrossRef](#)]
30. Kumar, M.; Singh, A.K.; Sikandar, M. Study of Sorption and Desorption of Cd (II) from Aqueous Solution Using Isolated Green Algae *Chlorella vulgaris*. *Appl. Water Sci.* **2018**, *8*, 225. [[CrossRef](#)]
31. Rinanti, A. Improving biosorption of Cu(II)-ion on artificial wastewater by immobilized biosorbent of tropical microalgae. *Geomate* **2017**, *13*, 6–10. [[CrossRef](#)]
32. Cheng, S.Y.; Show, P.-L.; Lau, B.F.; Chang, J.-S.; Ling, T.C. New Prospects for Modified Algae in Heavy Metal Adsorption. *Trends Biotechnol.* **2019**, *37*, 1255–1268. [[CrossRef](#)] [[PubMed](#)]
33. Fasaee, F.; Bitter, J.H.; Slegers, P.M.; Van Boxtel, A.J.B. Techno-Economic Evaluation of Microalgae Harvesting and Dewatering Systems. *Algal Res.* **2018**, *31*, 347–362. [[CrossRef](#)]
34. Salam, K.A. Towards sustainable development of microalgal biosorption for treating effluents containing heavy metals. *Biofuel Res. J.* **2019**, *6*, 948–961. [[CrossRef](#)]
35. Tüzün, İ.; Bayramoğlu, G.; Yalçın, E.; Başaran, G.; Çelik, G.; Arıca, M.Y. Equilibrium and Kinetic Studies on Biosorption of Hg(II), Cd(II) and Pb(II) Ions onto Microalgae *Chlamydomonas reinhardtii*. *J. Environ. Manag.* **2005**, *77*, 85–92. [[CrossRef](#)]
36. Ferreira, L.S.; Rodrigues, M.S.; de Carvalho, J.C.M.; Lodi, A.; Finocchio, E.; Perego, P.; Converti, A. Adsorption of Ni²⁺, Zn²⁺ and Pb²⁺ onto Dry Biomass of *Arthrospira (Spirulina) Platensis* and *Chlorella vulgaris*. I. Single Metal Systems. *Chem. Eng. J.* **2011**, *173*, 326–333. [[CrossRef](#)]
37. Flouty, R.; Estephane, G. Bioaccumulation and Biosorption of Copper and Lead by a Unicellular Algae *Chlamydomonas reinhardtii* in Single and Binary Metal Systems: A Comparative Study. *J. Environ. Manag.* **2012**, *111*, 106–114. [[CrossRef](#)] [[PubMed](#)]
38. Cheng, J.; Yin, W.; Chang, Z.; Lundholm, N.; Jiang, Z. Biosorption Capacity and Kinetics of Cadmium(II) on Live and Dead *Chlorella vulgaris*. *J. Appl. Phycol.* **2017**, *29*, 211–221. [[CrossRef](#)]
39. Saavedra, R.; Muñoz, R.; Taboada, M.E.; Vega, M.; Bolado, S. Comparative Uptake Study of Arsenic, Boron, Copper, Manganese and Zinc from Water by Different Green Microalgae. *Bioresour. Technol.* **2018**, *263*, 49–57. [[CrossRef](#)] [[PubMed](#)]
40. Pradhan, D.; Sukla, L.B.; Mishra, B.B.; Devi, N. Biosorption for Removal of Hexavalent Chromium Using Microalgae *Scenedesmus* sp. *J. Clean. Prod.* **2019**, *209*, 617–629. [[CrossRef](#)]
41. Tunali, M.; Yenigun, O. Biosorption of Ag⁺ and Nd³⁺ from Single- and Multi-Metal Solutions (Ag⁺, Nd³⁺, and Au³⁺) by Using Living and Dried Microalgae. *J. Mater. Cycles Waste Manag.* **2021**, *23*, 764–777. [[CrossRef](#)]
42. Mohamed, M.S.; Hozayen, W.; Alharbi, R.M.; Ibraheem, B.I.B.M. Adsorptive Recovery of Arsenic (III) Ions from Aqueous Solutions Using Dried *Chlamydomonas* sp. *Heliyon* **2022**, *8*, 20. [[CrossRef](#)]
43. Raji, Z.; Karim, A.; Karam, A.; Khalloufi, S. Adsorption of Heavy Metals: Mechanisms, Kinetics, and Applications of Various Adsorbents in Wastewater Remediation—A Review. *Waste* **2023**, *1*, 775–805. [[CrossRef](#)]
44. Xiao, X.; Li, W.; Jin, M.; Zhang, L.; Qin, L.; Geng, W. Responses and Tolerance Mechanisms of Microalgae to Heavy Metal Stress: A Review. *Mar. Environ. Res.* **2023**, *183*, 105805. [[CrossRef](#)] [[PubMed](#)]
45. Abdelfattah, A.; Ali, S.S.; Ramadan, H.; El-Aswar, E.I.; Eltawab, R.; Ho, S.-H.; Elsamahy, T.; Li, S.; El-Sheekh, M.M.; Schagerl, M.; et al. Microalgae-Based Wastewater Treatment: Mechanisms, Challenges, Recent Advances, and Future Prospects. *Environ. Sci. Ecotechnol.* **2023**, *13*, 100205. [[CrossRef](#)] [[PubMed](#)]
46. European Commission. *EIPPCB Reference Document on the Best Available Techniques for the Surface Treatment of Metals and Plastics*; European Commission: Brussels, Belgium, 2006.
47. European Commission. *EIPPCB Reference Document on the Best Available Techniques for the Ceramic Manufacturing Industry*; European Commission: Brussels, Belgium, 2007.
48. European Commission. *EIPPCB Reference Document on the Best Available Techniques for the Ferrous Metals Processing Industry*; European Commission: Brussels, Belgium, 2022.
49. European Commission. *UE Directive (EU) 2020/2184 of the European Parliament and of the Council of 16 December 2020 on the Quality of Water Intended for Human Consumption (Recast)*; European Commission: Brussels, Belgium, 2020.
50. Puigdomenech, I. *Hydra-Medusa Software, version 0.1.1*; Chemical Equilibrium Diagrams; KTH Royal Institute of Technology: Stockholm, Sweden, 2020.
51. Barth, A. Infrared Spectroscopy of Proteins. *Biochim. Biophys. Acta (BBA)—Bioenerg.* **2007**, *1767*, 1073–1101. [[CrossRef](#)] [[PubMed](#)]
52. Dean, A.P.; Nicholson, J.M.; Sigeo, D.C. Impact of Phosphorus Quota and Growth Phase on Carbon Allocation in *Chlamydomonas reinhardtii*: An FTIR Microspectroscopy Study. *Eur. J. Phycol.* **2008**, *43*, 345–354. [[CrossRef](#)]

53. Miller, D.H.; Lamport, D.T.A.; Miller, M. Hydroxyproline Heterooligosaccharides in *Chlamydomonas*. *Science* **1972**, *176*, 918–920. [[CrossRef](#)] [[PubMed](#)]
54. Adair, W.S.; Apt, K.E. Cell Wall Regeneration in *Chlamydomonas*: Accumulation of mRNAs Encoding Cell Wall Hydroxyproline-Rich Glycoproteins. *Proc. Natl. Acad. Sci. USA* **1990**, *87*, 7355–7359. [[CrossRef](#)] [[PubMed](#)]
55. Zheng, H.; Yin, J.; Gao, Z.; Huang, H.; Ji, X.; Dou, C. Disruption of *Chlorella vulgaris* Cells for the Release of Biodiesel-Producing Lipids: A Comparison of Grinding, Ultrasonication, Bead Milling, Enzymatic Lysis, and Microwaves. *Appl. Biochem. Biotechnol.* **2011**, *164*, 1215–1224. [[CrossRef](#)] [[PubMed](#)]
56. Romera, E.; González, F.; Ballester, A.; Blázquez, M.L.; Muñoz, J.A. Comparative Study of Biosorption of Heavy Metals Using Different Types of Algae. *Bioresour. Technol.* **2007**, *98*, 3344–3353. [[CrossRef](#)] [[PubMed](#)]
57. Areco, M.M.; Hanela, S.; Duran, J.; dos Santos Afonso, M. Biosorption of Cu(II), Zn(II), Cd(II) and Pb(II) by Dead Biomasses of Green Alga *Ulva Lactuca* and the Development of a Sustainable Matrix for Adsorption Implementation. *J. Hazard. Mater.* **2012**, *213–214*, 123–132. [[CrossRef](#)]
58. Sulaymon, A.H.; Mohammed, A.A.; Al-Musawi, T.J. Competitive Biosorption of Lead, Cadmium, Copper, and Arsenic Ions Using Algae. *Environ. Sci. Pollut. Res.* **2013**, *20*, 3011–3023. [[CrossRef](#)] [[PubMed](#)]
59. Harrison, G.I.; Campbell, P.G.C.; Tessier, A. Effects of pH Changes on Zinc Uptake by *Chlamydomonas variabilis* Grown in Batch Culture. *Can. J. Fish. Aquat. Sci.* **1986**, *43*, 687–693. [[CrossRef](#)]
60. Macfie, S.M.; Tarmohamed, Y.; Welbourn, P.M. Effects of Cadmium, Cobalt, Copper, and Nickel on Growth of the Green Alga *Chlamydomonas reinhardtii*: The Influences of the Cell Wall and pH. *Arch. Environ. Contam. Toxicol.* **1994**, *27*, 454–458. [[CrossRef](#)]
61. Melhi, S.; Ullah Jan, S.; Khan, A.A.; Badshah, K.; Ullah, S.; Bostan, B.; Selamoglu, Z. Remediation of Cd (II) Ion from an Aqueous Solution by a Starch-Based Activated Carbon: Experimental and Density Functional Theory (DFT) Approach. *Crystals* **2022**, *12*, 189. [[CrossRef](#)]
62. Persson, I.; Lyczko, K.; Lundberg, D.; Eriksson, L.; Placzek, A. Coordination Chemistry Study of Hydrated and Solvated Lead(II) Ions in Solution and Solid State. *Inorg. Chem.* **2011**, *50*, 1058–1072. [[CrossRef](#)] [[PubMed](#)]
63. Yuan, X.; Zhang, C. Density Functional Theory Study on the Inner Shell of Hydrated $M^{2+}(H_2O)_{1-7}$ Cluster Ions for $M = Zn, Cd$ and Hg . *Comput. Theor. Chem.* **2020**, *1171*, 112666. [[CrossRef](#)]
64. Treadwell, F.P. *Chimica Analitica Vol. 1 Analisi Qualitativa*, 7th ed.; Dr. Francesco Vallardi: Milano, Italy, 1966.
65. Crozza, D. Studio dei Meccanismi della Metallotolleranza Nell'organismo Modello *Scenedesmus acutus* (Chlorophyta—*Algae verdi*). Ph.D Thesis, Università della Calabria, Catanzaro, Italy, 2013.
66. Keller, A.A.; Wang, H.; Zhou, D.; Lenihan, H.S.; Cherr, G.; Cardinale, B.J.; Miller, R.; Ji, Z. Stability and Aggregation of Metal Oxide Nanoparticles in Natural Aqueous Matrices. *Environ. Sci. Technol.* **2010**, *44*, 1962–1967. [[CrossRef](#)]
67. Serrão Sousa, V.; Ribau Teixeira, M. Aggregation Kinetics and Surface Charge of CuO Nanoparticles: The Influence of pH, Ionic Strength and Humic Acids. *Environ. Chem.* **2013**, *10*, 313–322. [[CrossRef](#)]

Disclaimer/Publisher's Note: The statements, opinions and data contained in all publications are solely those of the individual author(s) and contributor(s) and not of MDPI and/or the editor(s). MDPI and/or the editor(s) disclaim responsibility for any injury to people or property resulting from any ideas, methods, instructions or products referred to in the content.